Evaluation of non-thermal plasma-induced anticancer effects on human colon cancer cells

JAE-SUN CHOI,[1,5] JEONGHO KIM,[2,5] YOUNG-JUN HONG,[3] WOOM-YEE BAE,[1] EUN HA CHOI,[3] JOO-WON JEONG,[1,4,6] AND HUN-KUK PARK[2,7]

[1]*Department of Biomedical Science, Graduate School, Kyung Hee University, Seoul 02447, South Korea*
[2]*Department of Biomedical Engineering, College of Medicine, Kyung Hee University, Seoul 02447, South Korea*
[3]*Plasma Bioscience Research Center, Kwangwoon University, Seoul 01897, South Korea*
[4]*Department of Anatomy and Neurobiology, College of Medicine, Kyung Hee University, Seoul 02447, South Korea*
[5]*Equal Contribution*
[6]*jjeong@khu.ac.kr*
[7]*sigmoidus@khu.ac.kr*

Abstract: Non-thermal atmospheric-pressure plasma has been introduced in various applications such as sterilization, wound healing, blood coagulation, and other biomedical applications. The most attractive application of non-thermal atmospheric-pressure plasma is in cancer treatment, where the plasma is used to produce reactive oxygen species (ROS) to facilitate cell apoptosis. We investigate the effects of different durations of exposure to dielectric-barrier discharge (DBD) plasma on colon cancer cells using measurement of cell viability and ROS levels, western blot, immunocytochemistry, and Raman spectroscopy. Our results suggest that different kinds of plasma-treated cells can be differentiated from control cells using the Raman data.

References and links

1. S. U. Kalghatgi, G. Fridman, M. Cooper, G. Nagaraj, M. Peddinghaus, M. Balasubramanian, V. N. Vasilets, A. F. Gutsol, A. Fridman, and G. Friedman, "Mechanism of blood coagulation by nonthermal atmospheric pressure dielectric barrier discharge plasma," IEEE Trans. Plasma Sci. **35**(5), 1559–1566 (2007).
2. B. Haertel, T. von Woedtke, K. D. Weltmann, and U. Lindequist, "Non-thermal atmospheric-pressure plasma possible application in wound healing," Biomol. Ther. (Seoul) **22**(6), 477–490 (2014).
3. G. Fridman, M. Peddinghaus, M. Balasubramanian, H. Ayan, A. Fridman, A. Gutsol, and A. Brooks, "Blood coagulation and living tissue sterilization by floating-electrode dielectric barrier discharge in air," Plasma Chem. Plasma Process. **26**(4), 425–442 (2006).
4. Y. Li, A. Kojtari, G. Friedman, A. D. Brooks, A. Fridman, and H. F. Ji, "Decomposition of L-Valine under Nonthermal Dielectric Barrier Discharge Plasma," J. Phys. Chem. B **118**(6), 1612–1620 (2014).
5. P. Y. Oh, J. H. Kim, Y. Hong, S. H. Cho, G. Cho, and E. H. Choi, "Spatiotemporal behavior of excited xenon-atom density in accordance with xenon mole fraction to neon in alternating-current plasma display panels by laser-absorption spectroscopy," IEEE Trans. Plasma Sci. **36**(3), 816–820 (2008).
6. N. K. Kaushik, N. Kaushik, B. Min, K. H. Choi, Y. J. Hong, V. Miller, A. Fridman, and E. H. Choi, "Cytotoxic macrophage-released tumour necrosis factor-alpha (TNF-α) as a killing mechanism for cancer cell death after cold plasma activation," J. Phys. D Appl. Phys. **49**(8), 084001 (2016).
7. J. H. Park, N. Kumar, D. H. Park, M. Yusupov, E. C. Neyts, C. C. Verlackt, A. Bogaerts, M. H. Kang, H. S. Uhm, E. H. Choi, and P. Attri, "A comparative study for the inactivation of multidrug resistance bacteria using dielectric barrier discharge and nano-second pulsed plasma," Sci. Rep. **5**(1), 13849 (2015).
8. N. K. Kaushik, P. Attri, N. Kaushik, and E. H. Choi, "A preliminary study of the effect of DBD plasma and osmolytes on T98G brain cancer and HEK non-malignant cells," Molecules **18**(5), 4917–4928 (2013).
9. W. Van Gaens and A. Bogaerts, "Kinetic modelling for an atmospheric pressure argon plasma jet in humid air," J. Phys. D Appl. Phys. **46**(27), 275201 (2013).

10. U. Kogelschatz, "Dielectric-barrier discharges: their history, discharge physics, and industrial applications," Plasma Chem. Plasma Process. **23**(1), 1–46 (2003).

11. H. Halfmann, N. Bibinov, J. Wunderlich, and P. Awakowicz, "A double inductively coupled plasma for sterilization of medical devices," J. Phys. D Appl. Phys. **40**(14), 4145–4154 (2007).

12. M. H. Ngo Thi, P. L. Shao, J. D. Liao, C. C. K. Lin, and H. K. Yip, "Enhancement of Angiogenesis and Epithelialization Processes in Mice with Burn Wounds through ROS/RNS Signals Generated by Non-Thermal N2/Ar Micro-Plasma," Plasma Process. Polym. **11**(11), 1076–1088 (2014).

13. P. L. Shao, J. D. Liao, T. W. Wong, Y. C. Wang, S. Leu, and H. K. Yip, "Enhancement of Wound Healing by Non-Thermal N2/Ar Micro-Plasma Exposure in Mice with Fractional-CO2-Laser-Induced Wounds," PLoS One **11**(6), e0156699 (2016).

14. S. Kalghatgi, C. M. Kelly, E. Cerchar, B. Torabi, O. Alekseev, A. Fridman, G. Friedman, and J. Azizkhan-Clifford, "Effects of non-thermal plasma on mammalian cells," PLoS One **6**(1), e16270 (2011).

15. G. Fridman, A. Shereshevsky, M. M. Jost, A. D. Brooks, A. Fridman, A. Gutsol, V. Vasilets, and G. Friedman, "Floating electrode dielectric barrier discharge plasma in air promoting apoptotic behavior in melanoma skin cancer cell lines," Plasma Chem. Plasma Process. **27**(2), 163–176 (2007).

16. C. H. Kim, J. H. Bahn, S. H. Lee, G. Y. Kim, S. I. Jun, K. Lee, and S. J. Baek, "Induction of cell growth arrest by atmospheric non-thermal plasma in colorectal cancer cells," J. Biotechnol. **150**(4), 530–538 (2010).

17. S. J. Kim, T. Chung, S. Bae, and S. Leem, "Induction of apoptosis in human breast cancer cells by a pulsed atmospheric pressure plasma jet," Appl. Phys. Lett. **97**(2), 023702 (2010).

18. B. Haertel, M. Hähnel, S. Blackert, K. Wende, T. von Woedtke, and U. Lindequist, "Surface molecules on HaCaT keratinocytes after interaction with non-thermal atmospheric pressure plasma," Cell Biol. Int. **36**(12), 1217–1222 (2012).

19. N. K. Kaushik, H. Uhm, and E. H. Choi, "Micronucleus formation induced by dielectric barrier discharge plasma exposure in brain cancer cells," Appl. Phys. Lett. **100**(8), 084102 (2012).

20. G. Kim, W. Kim, K. Kim, and J. Lee, "DNA damage and mitochondria dysfunction in cell apoptosis induced by nonthermal air plasma," Appl. Phys. Lett. **96**(2), 021502 (2010).

21. M. Ushio-Fukai and R. W. Alexander, "Reactive oxygen species as mediators of angiogenesis signaling: role of NAD(P)H oxidase," Mol. Cell. Biochem. **264**(1-2), 85–97 (2004).

22. K. P. Arjunan, G. Friedman, A. Fridman, and A. M. Clyne, "Non-thermal dielectric barrier discharge plasma induces angiogenesis through reactive oxygen species," J. R. Soc. Interface **9**(66), 147–157 (2012).

23. S. Kalghatgi, A. Fridman, J. Azizkhan Clifford, and G. Friedman, "DNA Damage in Mammalian Cells by Non-thermal Atmospheric Pressure Microsecond Pulsed Dielectric Barrier Discharge Plasma is not Mediated by Ozone," Plasma Process. Polym. **9**(7), 726–732 (2012).

24. K. D. Jacob, N. Noren Hooten, A. R. Trzeciak, and M. K. Evans, "Markers of oxidant stress that are clinically relevant in aging and age-related disease," Mech. Ageing Dev. **134**(3-4), 139–157 (2013).

25. P. Morales-Ramírez, V. Cruz-Vallejo, R. Peña-Eguiluz, R. López-Callejas, B. G. Rodríguez-Méndez, R. Valencia-Alvarado, A. Mercado-Cabrera, and A. E. Muñoz-Castro, "Assessing cellular DNA damage from a helium plasma needle," Radiat. Res. **179**(6), 669–673 (2013).

26. A. Sinha, T. T. Chu, M. Dao, and R. Chandramohanadas, "Single-cell evaluation of red blood cell bio-mechanical and nano-structural alterations upon chemically induced oxidative stress," Sci. Rep. **5**(1), 9768 (2015).

27. T. Furuhashi, Basics of Multivariate Analysis II (Principal Component Analysis): Theory and Exercise using R (Amazon Digital Services LLC, 2015).

28. T. Furuhashi, Basics of Multivariate Analysis III (Discriminant Analysis): Theory and Exercise using R (Amazon Digital Services LLC, 2016).

29. "The R Project for Statistical Computing", retrieved September 21, 2016, https://www.r-project.org.

30. K. Panngom, K. Y. Baik, M. K. Nam, J. H. Han, H. Rhim, and E. H. Choi, "Preferential killing of human lung cancer cell lines with mitochondrial dysfunction by nonthermal dielectric barrier discharge plasma," Cell Death Dis. **4**(5), e642 (2013).

31. W. T. Chang, H. L. Lin, H. C. Chen, Y. M. Wu, W. J. Chen, Y. T. Lee, and I. Liau, "Real-time molecular assessment on oxidative injury of single cells using Raman spectroscopy," J. Raman Spectrosc. **40**(9), 1194–1199 (2009).

32. G. B. Jung, Y. J. Lee, G. Lee, and H.-K. Park, "A simple and rapid detection of tissue adhesive-induced biochemical changes in cells and DNA using Raman spectroscopy," Biomed. Opt. Express **4**(11), 2673–2682 (2013).

33. N. Kaushik, S. J. Lee, T. G. Choi, K. Y. Baik, H. S. Uhm, C. H. Kim, N. K. Kaushik, and E. H. Choi, "Non-thermal plasma with 2-deoxy-D-glucose synergistically induces cell death by targeting glycolysis in blood cancer cells," Sci. Rep. **5**, 8726 (2015).

34. Y. Ma, C. S. Ha, S. W. Hwang, H. J. Lee, G. C. Kim, K. W. Lee, and K. Song, "Non-thermal atmospheric pressure plasma preferentially induces apoptosis in p53-mutated cancer cells by activating ROS stress-response pathways," PLoS One **9**(4), e91947 (2014).

35. E. Panieri and M. M. Santoro, "ROS homeostasis and metabolism: a dangerous liason in cancer cells," Cell Death Dis. **7**(6), e2253 (2016).

36. M. Podhorecka, A. Skladanowski, and P. Bozko, "H2AX phosphorylation: its role in DNA damage response and cancer therapy," J. Nucleic Acids **2010**, 920161 (2010).

37. A. Gross, J. M. McDonnell, and S. J. Korsmeyer, "BCL-2 family members and the mitochondria in apoptosis," Genes Dev. **13**(15), 1899–1911 (1999).
38. A. G. Porter and R. U. Jänicke, "Emerging roles of caspase-3 in apoptosis," Cell Death Differ. **6**(2), 99–104 (1999).
39. S. N. Zucker, J. Zirnheld, A. Bagati, T. M. DiSanto, B. Des Soye, J. A. Wawrzyniak, K. Etemadi, M. Nikiforov, and R. Berezney, "Preferential induction of apoptotic cell death in melanoma cells as compared with normal keratinocytes using a non-thermal plasma torch," Cancer Biol. Ther. **13**(13), 1299–1306 (2012).
40. K. Panngom, K. Y. Baik, M. K. Nam, J. H. Han, H. Rhim, and E. H. Choi, "Preferential killing of human lung cancer cell lines with mitochondrial dysfunction by nonthermal dielectric barrier discharge plasma," Cell Death Dis. **4**(5), e642 (2013).
41. H. Tanaka, M. Mizuno, K. Ishikawa, K. Nakamura, H. Kajiyama, H. Kano, F. Kikkawa, and M. Hori, "Plasma-Activated Medium Selectively Kills Glioblastoma Brain Tumor Cells by Down-Regulating a Survival Signaling Molecule, AKT Kinase," Plasma Medicine **1**(3-4), 265–277 (2011).
42. S. Iseki, K. Nakamura, M. Hayashi, H. Tanaka, H. Kondo, H. Kajiyama, H. Kano, F. Kikkawa, and M. Hori, "Selective killing of ovarian cancer cells through induction of apoptosis by nonequilibrium atmospheric pressure plasma," Appl. Phys. Lett. **100**(11), 113702 (2012).

1. Introduction

Plasma is regarded as the fourth state of matter formed by ionized gas-applied electrical energy. Over the last year, non-thermal atmospheric-pressure plasma has emerged as a promising tool for use in various applications such as sterilization of infected tissues, wound healing, blood coagulation, and delicate surgery [1–3]. Among these, the most attractive and the most extensively studied application is in the treatment of cancer, which is a leading cause of death in humans. Non-thermal atmospheric-pressure plasma is suitable for treatment of living cells as its temperature is close to the room temperature, because of which it does not burn these cells [1].

Non-thermal atmospheric pressure dielectric-barrier discharge (DBD) plasma is one of the most suitable candidates for use as a bio-medical device [4]. In the recent years, DBD was mainly used for alternating-current plasma display panels (AC-PDPs) with micro-gap electrodes (a few tens to a few hundreds of micrometers) [5]. Many plasma researchers have focused on the optimization of different aspects of AC-PDPs, such as the electrode structure, gas pressure, and mixing conditions of rare gases [5]. Recently, DBDs with micro-gap electrodes have used in various industries and biology fields. Customized DBD sources for stable living cell treatment have also been developed at the PBRC (plasma bioscience research center) of Kwangwoon University in Korea [6,7]. In particular, these plasmas have many advantages for biomedical applications, because DBD plasma sources provide a large contact area for the samples and have an optimum temperature for sensitive living tissues.

Atmospheric-pressure plasma generates excited atoms, charged particles such like electrons and ions, chemical radicals, and photons (ultraviolet, infrared, etc.) [8]. Many researchers have studied radical species dynamics in non-thermal plasma. A computer simulation revealed that an Argon plasma jet in humid air could generate O_3, reactive oxygen species (ROS), and reactive nitrogen species (RNS) [9], which were found to be biomedically active molecules. In particular, non-thermal atmospheric-pressure DBD plasma can generate ozone gases for a long time [10]. In the case of narrow discharge as in micro-gap DBD plasmas, it is preferable to generate ozone for an atmospheric pressure environment [10]. The plasma conditions in the microdischarges also need to be optimized for excited and dissociating oxygen and nitrogen molecules [10]. In particular, ozone is formed in a three-body reaction involving O and O_2 ($O + O_2 + M \rightarrow O_3^* + M \rightarrow O_3 + M$; M: 3rd collision partner) [10]. Because ozone is a molecule with a strong sterilizing and oxidation effect, DBDs with micro-gap electrodes are important candidates for use as a medical device for large wound healing and blood coagulation in the human body.

Atmospheric-pressure non-thermal plasma produces ROS by electron excitation of the working gas [2, 11, 12]. Various groups have reported that the produced ROS influence cell proliferation in vitro [13, 14]. It is also known that plasma treatment improves cancer therapy by inducing apoptosis and growth arrest of tumor cells [15–18]. ROS induce apoptosis

through DNA damage and mitochondrial dysfunction in cancer cell lines [19,20]. Although low doses of ROS may improve downstream signals of growth factors and promote cell proliferation, non-thermal plasma could cause dose-dependent DNA damage in mammalian cells in culture media [20–23]. This oxidative harm is also considered to trigger advanced aging and senescence of red blood cells (RBCs) or leukocytes [24, 25]. As RBCs contain a lipid bilayer and circulate ubiquitously, they are vulnerable to oxidative stress, which leads to the alteration of membrane potential and permeability. This causes deformability of the RBCs and ultimately causes hemolysis [26].

The purpose of our study was to differentiate between plasma-treated cells and control cells using Raman spectral data examined with principal component analysis-discriminant analysis (PCA-DA) and to correlate the Raman data with biological results obtained using the MTT assay, measurement of ROS, western blot, and immunocytochemistry. The PCA-DA performed using Raman spectroscopy showed that the plasma-treated cells could be distinguished with high sensitivity and specificity. Therefore, we believe that measurements of Raman spectroscopy data with PCA-DA could provide another useful method for elucidating the mechanisms underlying the effects of various kinds of cold plasma on some cells.
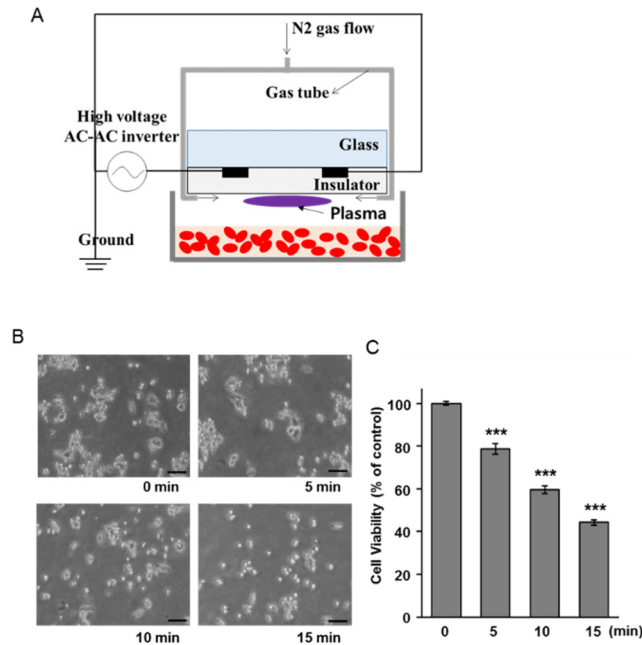

Fig. 1. Anticancer effects of non-thermal plasma on HCT116 cells. (A) Schematic diagram of non-thermal plasma treatment. (B) The microscopic images of HCT116 cells at 24 h after plasma exposure. Scale bar = 100 μm. (C) MTT assay was performed using cells at 24 h after specific treatment. The data are presented as the mean ± SEM. *** denotes p < 0.001 compared to the unexposed cells.

2. Materials and methods

2.1 Reagents and antibodies

We used 3-[4,5-dimethylthiazol-2-yl]-2,5-diphenyl tetrazolium bromide (MTT) and Hoechst 33342 (Sigma-Aldrich, St. Louis, MO, USA); 5,6-carboxy-2′,7′-dichlorofluorescein diacetate (H2DCF-DA); and MitoSox red (Thermo Fisher Scientific, Eugene, OR, USA). We also used antibodies against Bax, Bcl2, and p53 (Santa Cruz Biotechnology, Santa Cruz, CA, USA), α-tubulin (Sigma-Aldrich), and phospho-γ-H2AX (Cell Signaling, Beverly, MA, USA).

2.2 Non-thermal dielectric discharge plasma device

The non-thermal DBD plasma (model name: ϕ35 cm μ-DBD, Plasma Bioscience Research Center of Kwangwoon University, Seoul, Korea) consisted of many electrodes composed of silver material covered with an insulator below the glass plate (Fig. 1(A)). Ninety-five electrodes with a gap distance of 100 μm of this DBD plasma device were covered with the insulator of 50-μm thickness. DBD plasma was generated in the area between these small gaps on the surface of the insulator. The electrodes were then applied by a high voltage pulse in a DC-AC inverter, which could generate a dimming pulse with 22 kHz as the main operating frequency. The average voltage and current were about 1.16 kV and 2.8 mA, respectively. We used the nitrogen (N_2) DBD plasma with a gas flow rate of 1.5 L/min. The DBD plasma source could be inserted into a Petri dish containing cell suspensions, thus ensuring that plasma source does not come in direct contact with the cells.

2.3 Cell culture and plasma treatment

Cells of the human colon cancer cell line, HCT116, were purchased from the American Type Culture Collection (ATCC, Rockville, MD, USA) and were maintained in RPMI1640 (Welgene, Korea) supplemented with 10% fetal bovine serum (HyClone, Thermo Fisher Scientific, Victoria, Australia) and 1% penicillin/streptomycin (Cellgro, Herndon, VA, USA) in a humidified 5% CO_2 incubator. For plasma treatment, we transferred 1.5 mL of the cell suspension (5×10^5 cells/mL) on a petri dish with 3.5 cm diameter (SPL, Korea) as described in Fig. 1(A). After plasma exposure for 5, 10, and 15 min, the cell suspension was divided into 24-well and 6-well culture plates for the subsequent experiments.

2.4 Measurement of cell viability

To measure cell viability, 24 h after specific plasma exposure, the MTT assay was performed according to the manufacturer's protocol. Absorption at 570 nm was normalized to that of untreated cells, and the data were expressed cellular viability as a percentage of that of the control cells. All the values were expressed as the mean ± standard error of the mean (SEM) of three wells from three independent experiments. Student's t test was used for the analysis of significance of the differences between the data sets.

2.5 Immunofluorescence staining

Twenty-four hours after plasma treatment, the cells were fixed with 4% paraformaldehyde solution for 15 min and then permeabilized with 0.5% Triton X-100 for 15 min. The cells were then incubated with anti-p-γ-H2AX antibody at 4°C overnight, followed by incubation with Alexa 488-conjugated anti-rabbit antibody (Invitrogen) for 1 h. The nuclei were counterstained with Hoechst 33342 for 10 min. The fluorescent signal was then examined under confocal microscopy (LSM700; Carl Zeiss, Oberkochen, Germany).

2.6 Detection of intercellular and mitochondrial ROS

To quantitate the ROS, we incubated the cells with 0.5 μM H2DCF-DA and 1 μM MitoSox for 30 min and 15 min, respectively, and the fluorescent signal was then quickly examined using a fluorescence microscope (Axioskop2, Carl Zeiss).

2.7 Preparation of cell extracts and western blotting

The cells were lysed using NP-40 lysis buffer (10 mM Tris, 10 mM NaCl and 0.2% NP-40) containing a protease inhibitor cocktail (Sigma-Aldrich) and phosphatase inhibitors (1 mM Na_3VO_4 and 10 mM NaF). For immunoblotting, total proteins were separated by SDS-PAGE and then transferred onto a PVDF membrane (Millipore Corporation, Billerica, MA, USA). The membranes were blocked with Tris-buffered saline containing 0.1% Tween 20 (TBS-T) and incubated with primary antibodies diluted in blocking buffer overnight at 4°C. The

membranes were then washed and incubated with the appropriate HRP-conjugated secondary antibodies (Vector Laboratories, Burlingame, CA, USA) for 1 h at room temperature. The signal was detected using an ECL Western detection system (Thermo Scientific, Rockford, IL, USA).

2.8 Raman spectroscopy

The control and plasma-treated cells were fixed using 4% paraformaldehyde for 30 min at 37°C and 5% humidity in an incubator and washed three times using PBS for 10 min before Raman measurements. The cells were then rinsed with distilled water 10 times to avoid Raman peaks of the PBS. Ten microliters of each sample (control cells and cells exposed to the DBD over 15 min) was dropped and dried on an SERS substrate (SILMECO, Copenhagen, Denmark). Raman spectra obtained using a spectroscope (BRUKO, GERMAN) with a diode laser beam at an excitation wavelength of 785 nm were acquired in the range of $417-1782$ cm^{-1} with a spectral resolution of 0.5 cm^{-1}. The laser source with a power of 10 mW with a $\times$ 50 object lens was focused on the SERS substrate with a spot diameter of ~2 μm and an acquisition time of 10 s. The procedure was repeated 50 times to measure the Raman spectra for each sample. A baseline correction was accomplished using the OPUS 7.1 software (Bruker Optics, Ettlingen, Germany). The data set was normalized with respect to the 1441 cm^{-1} band without smoothing. The mean Raman spectra and standard deviation were calculated and plotted from fifty normalized Raman spectra data for control and plasma-treated cells, respectively. The average was plotted as a solid line, while the standard deviation was presented as a filled area.

2.9 Multivariate and statistical analyses

PCA, which is known as one of multivariate methods, was applied to the Raman spectra of the control cells and the cells treated with plasma for 15 min to distinguish the spectral features between the two sets of samples. PCA is a statistical method used in a variety of fields and is a common technique for distinguishing patterns in data of high dimensions [27]. The spectra are analyzed by linear discriminant analysis (LDA) using the first eight principal components. Then, the sensitivity, specificity, and error are calculated for quantitative discrimination between the two groups. Sensitivity, specificity, and error are defined as TP/(TP + FN), TN/(TN + FP), and (FN + FP)/(FN + TN + FP + TP), respectively, where TP, TN, FP, and FN present the number of true positives, the number of true negatives, the number of false positives, and number of false negatives, respectively [28]. We adopted the built-in R function prcomp and lda for PCA and LDA. R is a free software environment for statistical computation and graphics [29].
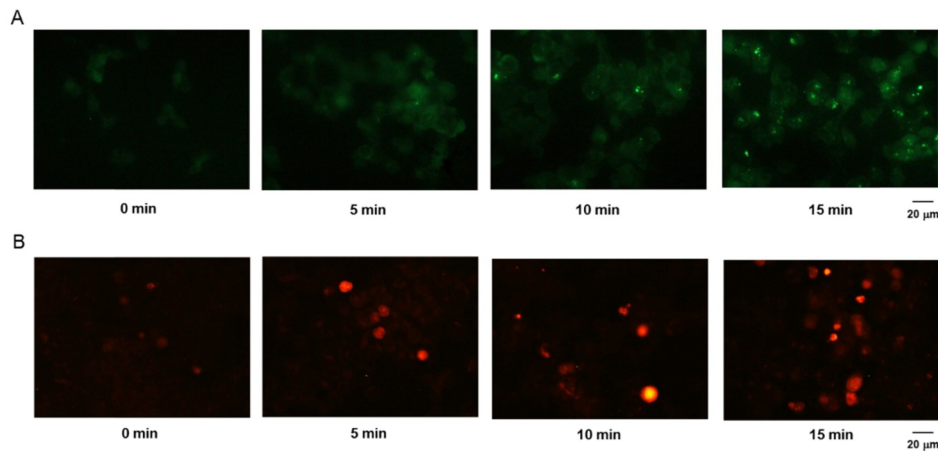
Fig. 2. Induction of ROS generation in non-thermal plasma-treated HCT116 cells. For measurement of intracellular and mitochondrial ROS levels, the plasma-treated cells were incubated with 0.5 μM of H2DCF-DA (A) and 1 μM of MitoSox (B) and examined under a fluorescence microscope. Scale bar = 20 μm.

3. Results

3.1 Non-thermal plasma has potent anticancer effects

Non-thermal DBD plasma has been shown to kill human lung cancer cells [30]. To confirm the anticancer effect of non-thermal plasma on human colon cancer cells, we treated the HCT116 cells with plasma. Figure 1(A) is a schematic diagram of the DBD plasma device used in this study. The plasma was applied to the cell suspensions in a petri dish for different exposure times of 5, 10, and 15 min. After plasma exposure, the morphology of the cells 24 h after exposure was examined by phase contrast microscopy. Their shape changed and the cell number clearly decreased with exposure time (Fig. 1(B)). Therefore, we investigated the effect of different exposure times to non-thermal plasma on HCT116 cells. As shown in Fig. 1(C), the viability of the HCT116 cells also significantly decreased in an exposure time-dependent manner. These results indicated that non-thermal plasma had anticancer effects on HCT116 cells.

3.2 Non-thermal plasma induces ROS generation

Because ROS have been reported to be involved in tumor cell death, we next investigated the effect of non-thermal plasma on the generation of ROS in tumor cells. The fluorescent probe H2DCF-DA was used to assess the generation of ROS. When the fluorescent signal was examined microscopically, we found that treatment with non-thermal plasma strongly increased intracellular ROS levels (Fig. 2(A)). In addition, to determine whether the ROS produced due to treatment with non-thermal plasma were generated in the mitochondria, we stained the non-thermal plasma-treated cells with MitoSox. We found that mitochondrial ROS levels were increased in the plasma-treated cells (Fig. 2(B)), which indicated that plasma treatment induced ROS generation by the mitochondria.
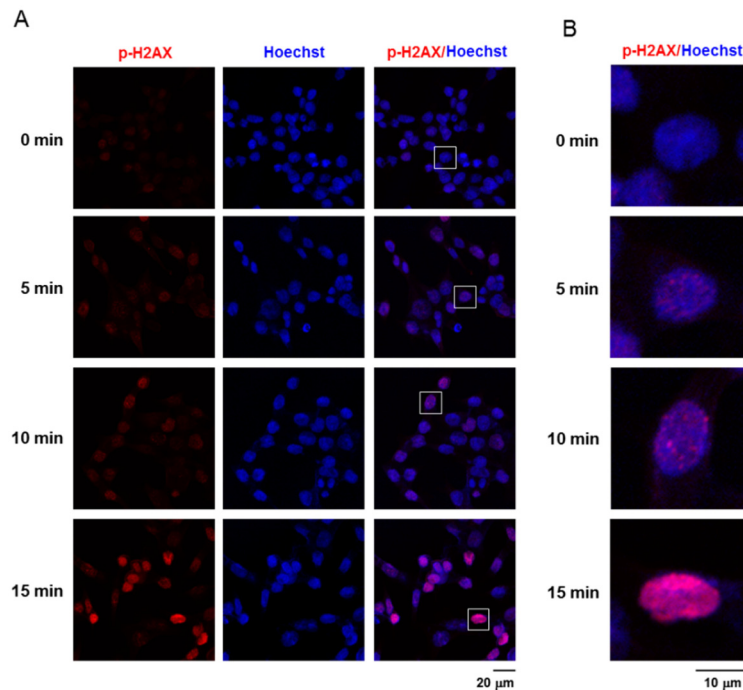
Fig. 3. Non-thermal plasma promotes DNA damage in the HCT116 cells. (A) Red represents stained γ-H2AX foci and blue represents stained nuclei in the plasma-treated HCT116 cells. Scale bar = 20 μm. (B) The inset of (A) was magnified under confocal microscope. Scale bar = 10 μm.

3.3 Non-thermal plasma increases DNA damage

In order to assess the DNA damage induced by treatment with non-thermal plasma, immuno-detection of the phosphorylated form of the histone H2AX was performed. As shown in Figs. 3(A) and (B), the foci formation of γ-H2AX in the plasma-treated cells was increased as compared to that in the unexposed cells. These results suggested that the time-dependent foci formation was associated with non-thermal plasma-induced death of the HCT116 cells.
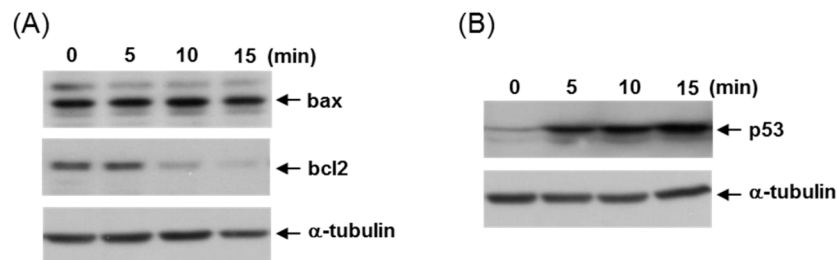

Fig. 4. Non-thermal plasma induces apoptotic cell death mediated by p53 activation. (A) Immunoblotting was performed using the total cell extract from HCT116 cells at 24 h after plasma exposure as indicated with antibodies against Bax, Bcl2, and α-tubulin. (B) Expression of p53 protein in these cells was examined by western blotting and α-tubulin protein served as a loading control.

3.4 Non-thermal plasma activates p53-mediated cell death signaling

Next, we investigated the activation of cell death signaling molecules in the non-thermal plasma-treated cells. Given that some cell death-induced genotoxic agents frequently signal by causing changes in the expression of Bax and Bcl2, we now decided to examine the

possible alterations in the levels of these two proteins. When the HCT116 cells were treated with plasma, the levels of anti-apoptotic Bcl2 protein decreased, whereas those of the pro-apoptotic Bax protein did not show any change (Fig. 4(A)). These data indicated that plasma treatment increased the Bax/Bcl2 ratio, which is the key regulator of apoptosis under conditions of stress. Because p53 can regulate the Bax/Bcl2 ratio in apoptotic cell death, we further examined the expression of p53. As shown in Fig. 4(B), levels of p53 protein increased upon treatment with non-thermal plasma, which suggested that plasma treatment increases the Bax/Bcl2 ratio, a pro-apoptotic switch, through the activation of p53 and thus induces apoptotic cell death.
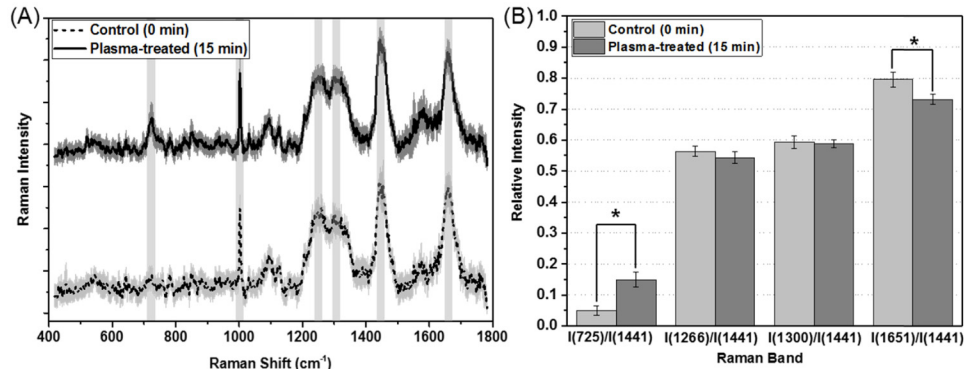

Fig. 5. (A) Raman spectra for the control cells and cells treated with plasma for 15 min. The thick lines show the average Raman spectra and the shaded areas represent standard deviations. (B) Relative intensities of the Raman bands of the control cells and the cells treated with plasma for 15 min. The data are presented as the mean ± SEM. Differences with p-values < 0.05 were considered statistically significant.

3.5 Raman measurements characterize representative peaks of the plasma-treated group

We considered six representative peaks for the control cells and those treated with plasma for 15 min (Fig. 5(A)). These peak assignments were identified as vibrations of the DNA base adenine, phenylalanine, CH bending, CH2 twisting, CH2 bending, and C = C stretching at 725, 1003, 1266, 1300, 1441, and 1651 cm^{-1}, respectively (Table 1). These tendencies were consistent with reports of previous studies in which the oxidative injury of single cells was investigated using Raman spectroscopy (Fig. 5(B)) [31, 32]. Three relative peak intensities were calculated for a comparison between the two groups at 725, 1651, 1266, and 1300 cm^{-1} with respect to that at 1441 cm^{-1}. The average values of I(725 cm^{-1})/I(1441 cm^{-1}) and I(1651 cm^{-1})/I(1441 cm^{-1}) for the cells treated with plasma for 15 min were 0.149 and 0.732, respectively, with the first group showing a significant increase of 195% and the second group showing a decrease of 8.1% compared to the control group (0.05 and 0.796). The other two relative intensities were similar to each other. This pattern was consistent with the results of the study conducted by Chang et al. [31]

Table 1. Assignments for the Raman peak positions of the control cells and the cells treated with plasma for 15 min.

Peak position	Assignments
725 cm^{-1}	Vibration of the DNA base adenine
1003 cm^{-1}	Phenylalanine
1266 cm^{-1}	CH bending
1300 cm^{-1}	CH$_2$ twisting
1441 cm^{-1}	CH$_2$ bending
1651 cm^{-1}	C = C stretching

Table 2. Classification results for Raman prediction of the two groups using a principal component analysis-linear discriminant analysis (PCA-LDA) algorithm, where 80% and 20% of the total data set were used for the training and test groups, respectively. The spectra were analyzed by linear discriminant analysis (LDA) using the first eight principal components.

		Calculated class	
		Control (N)	Plasma-treated (P)
Experimental class	Control (N)	8.369	0.131
	Plasma-treated (P)	1.631	9.869
	Sensitivity (%)	86.6	
	Specificity (%)	98.6	
	Accuracy (%)	91.2	
	Error (%)	8.8	

3.6 PCA-DA helps distinguish between the plasma-treated and control groups

As mentioned above, the patterns for the control and plasma-treated groups showed similarity, except for the peaks at 725 and 1651 cm^{-1}. Next, PCA-DA was introduced to quantitatively differentiate between the two groups using Raman data. First, we performed PCA for both the groups; the first eight principal components were then used for quantitative classification using linear discriminant analysis (LDA). We found that 80% of the total data set (fifty Raman data for each group) comprised the training data set used to find the discriminant function, which provided the predicted values for 20% of the total data set as the test data set. The training and test data sets were chosen randomly for 1000 iterations, and the classification results presented the average values for accuracy, sensitivity, and specificity, which were found to be 91%, 87%, and 99%, respectively (Table 2).

4. Discussion

The therapeutic potential of non-thermal plasma for cancer treatment has recently been reported. Many researchers have reported that treatment with non-thermal plasma induces cancer cell death by producing ROS [33, 34]. Our results also revealed that HCT116 cell death was induced upon treatment with non-thermal plasma (Fig. 1). Moreover, our findings revealed that non-thermal plasma treatment-induced production of ROS occurred in the mitochondria (Fig. 2). Increases in intracellular ROS production is known to cause cancer cell death through DNA damage [35]. In our study as well, we found that non-thermal plasma treatment induced γH2AX phosphorylation (Fig. 3), which is an early response to DNA damage in cells [36]. Additionally, we identified both the Bax/Bcl2 ratio and p53 expression were increased by non-thermal plasma treatment in the HCT116 cells (Fig. 4). Changes in these apoptosis-related proteins (p53, Bcl-2, and Bax) contribute to cell apoptosis through the caspase-3-dependent pathway [37]. The activation of caspase-3 has been observed during apoptotic cell death in many types of cancer cells in previous studies as well [38]. In addition, many researchers have reported that the tumor cell selectivity of non-thermal plasma was compared between normal cells and cancer cells such as skin cancer cells [39], lung cancer cells [40], glioma cells [41], and ovarian cancer cells [42]. From these previous reports, we suggest that non-thermal plasma specifically induces the oncogenic colon cell death or has mild effects on non-oncogenic cells.

The Raman spectroscopic measurements revealed six peaks at 725, 1003, 1266, 1300, 1441, and 1651 cm^{-1} for the control and plasma-treated groups. Two peaks at 725 and 1651 cm^{-1} were strikingly different between the two groups. The relative peak intensity of the group treated with plasma for 15 min was 8% less than that of the control group; this result was consistent with the report of Chang et al. [31] After exposure to hydroxyl radicals on single optically trapped liposomes or yeast, the reduction in peak intensity observed at 1651 cm^{-1} was found to be due to the peroxidation of the C = C bonds, which increases with

increasing concentrations of ROS. The Raman band observed at 725 cm^{-1} in our study is assigned to the adenine band of DNA [32]. The relative intensity of the group treated with plasma for 15 min was 195% higher than that of the control group, which indicated an increase in DNA damage owing to an increase in intracellular ROS production. This observation using Raman data correlated with the measured data of DNA damage of the HCT116 cells (Fig. 3).

The PCA-DA algorithm was greatly helpful in classifying Raman data for the comparison between the two groups. This discrimination result gave the best values for accuracy and sensitivity (91.2% and 86.6%, respectively). We considered the first eight principal components for LDA because of it provided better prediction capabilities than that achieved using the first three or up to seven principal components. The accuracy and sensitivity may be further improved by introducing non-LDA such as quadratic or orthogonal quadratic discriminant functions. In our future studies, we will focus on understanding the quantitative relationship between ROS production and the Raman intensities at 725 cm^{-1} and at 1651 cm^{-1} to investigate the degree of apoptotic cell death mediated by p53 activation as well as DNA damage.

5. Conclusions

We studied the degree of apoptosis in colon cancer cells upon treatment with DBD plasma for different times. We found that DBD plasma induced HCT116 cell death by increasing DNA damages and apoptosis. Measurements of Raman spectroscopy were also performed and the data were analyzed using PCA-DA to differentiate the plasma-treated cells from the control cells. The classification results showed accuracy, sensitivity, and specificity (91%, 87%, and 99%, respectively). Based on our findings, we believe that the use of Raman data with multivariate analysis can be useful as another analytical tool for studying various kinds of non-thermal atmospheric-pressure plasma that can be applicable in biomedical fields.

Funding